Lithuanian Journal of Physics, Vol. **62**, No. 1, pp. 21–43 (2022)

INTERPRETATION OF THE ANOMALOUS GROUNDWATER CHEMISTRY AND $^{234}U/^{238}U$ ACTIVITY RATIO DISEQUILIBRIUM IN THE NORTHERN PART OF THE BALTIC REGION

R. Mokrik and V. Samalavičius

Institute of Geosciences at Vilnius University, Čiurlionio 21/27, 03101 Vilnius, Lithuania
Email: robert.mokrik@gf.vu.lt; vytautas.samalavicius@chgf.vu.lt

Received 24 January 2021; revised 1 June 2021; accepted 21 September 2021

The anomalous isotope-hydrogeochemistry phenomena in the groundwater of Estonian Cambrian-Vendian (Ediacaran) and Ordovician-Cambrian aquifer systems were formed in the Late-Middle Pleistocene. In the periglacial environment, in northern and northwestern Estonia, these aquifer systems with fracture porose crystalline basement are connected to hydraulically joint unit characterized by high radioactivity groundwater. A significant alteration of groundwater occurred by series of isotope and chemistry facies fractionation. In this study, uranium isotopes activity ratio ($^{234}U/^{238}U$), ^{4}He content, isotope-hydrogeochemistry and adjusted ^{14}C ages are coupled for a new prospect of the estimation of northern Baltic Basin groundwater evolution. Analyzing radiocarbon and ^{4}He groundwater residence time results and uranium isotope activity ratio distribution suggests a prolonged periglacial environment in which groundwater evolved. Stable isotope ratios of $\delta^{18}O$ and $\delta^{2}H$ correlation and hydrochemical composition changes support the cryogenic origin of groundwater. Pleistocene glaciations cyclically affect groundwater in multiple ways: permafrost isotope-geochemistry partitioning; periodically changing reversed flow directions of recharge and discharge areas; oscillations of the sea, river system, and periglacial lakes level, surface and sub-permafrost water mixing via taliks and fractured basement rocks. These processes lead to forming the sequence of isotope-hydrogeochemistry types and specific zoning; in general, two separate groundwater fractions – brackish in the lower part and freshened above. An extensive groundwater exploitation on the northern coast sites influenced a sharp dysfunction in the groundwater body, destabilizing the natural equilibrium state formed in the Holocene and Pleistocene.

Keywords: Estonian Homocline, periglacial permafrost, cryogenic groundwater, isotope-geochemistry, groundwater dating

PACS: 91.67. Qr, 91.67.Rx, 92.40.Kf

1. Introduction

Periglacial permafrost formation directly influences the chemical and isotopic composition of groundwater or ground ice through cryogenesis, evidenced in the large areas in Siberia and Canada. Permafrost alteration of the isotope-geochemistry signature helps reconstruct the past environment and explain the chemical composition and evolution of paleogroundwater. Cryogenic fractionation of a stable $\delta^{18}O$ isotope in the ice-water system strongly depends on the freezing velocity [1]. Under equilibrium conditions, the fractionation constant for $\delta^{18}O$ is 2.8–3.0‰ [2–4]. In nature, freezing velocity determines whether fractionation occurs under kinetic or non-equilibrium conditions [5, 6]. A data set compiled from previous studies shows that $\delta^{18}O$ values of ground ice in Siberia, Canada and Alaska vary from –17 to –28‰ [7]. Fresh, brackish and saline groundwater explored in the Canadian Shield (depth up to 1300 m) were altered by freezing [8]. Due to cryogenic salt rejection, concentrations of the dissolved solids increase with depth in permafrost terrains. The stratification of groundwater chemical composition is a common indicator of cryogenesis: a gradual change of chemical facies from a bicarbonate to chloride type is observed with increasing depth due to changes in carbonate equilibrium and mineral precipitation [9–15].

The groundwater recharge/discharge formation during the Pleistocene glacial history is still uncertain. Several hypotheses were built up because highly depleted $\delta^{18}O$ values of groundwaters have been found in the Cambrian-Vendian and Ordovician-Cambrian aquifers systems on the Estonian Homocline (EH). The first was related to groundwater cryogenic metamorphization during permafrost formation based on stable and radioactive environmental isotope-geochemistry studies [16–19]. The first sampling campaign (14 boreholes) for radiocarbon (^{14}C) and helium (^{4}He) noble gas studies was executed in northern and eastern Estonia in 1974–1975 by the Lithuanian Geological Institute to assess groundwater resources and analyzed groundwater resources in the Radiocarbon Laboratory of the Institute. The Estonian Geological Survey made the second campaign from the 15 boreholes – in the Tallinn and Pärnu intakes during 1981–1982. Analyses were executed by the Isotope Laboratory of the Institute of Hydrogeology and Engineering Geology (Moscow). The northern part of Estonia Cm-V aquifer groundwater residence time, according to radiocarbon dating, varies from 7 to 33 ka [20–23]. Significantly younger (from 7 to 10 ka) groundwater was observed at buried valleys along the northern coast, where modern groundwater recharges. The groundwater age in the Voronka (V_2vr) and Gdov (V_2gd) aquifers (a subdivision of Cm-V formation) varies from the Gulf of Finland coast up to Alatskivi on the western part of the Peipus Lake – 17–27 and 23–33 ka, respectively [20].

Estonian researchers proposed a three end-member mixing model to explain the origin of the Estonian Cm-V and O-Cm groundwater as a consequence of glacial meltwater, crystalline basement brackish water mixing and modern groundwater recharge [24–29]. Another point of view suggests that the cryogenesis could explain the isotope-geochemistry anomaly because EH groundwater was strongly affected by permafrost [17, 18]. High $^{234}U/^{238}U$ activity ratio (AR) values support the groundwater permafrost origin [19].

The flow and mass transport modelling revealed that the available groundwater resources at the northern coast are limited. Due to the sea intrusion via the submarine part of buried valleys and the crystalline basement, cryogenically altered brackish groundwater inflow shows changing $\delta^{18}O$ background values and rising total dissolved solids (TDS) content up to 1.5 g/L [30]. Elevated Ra concentration throughout the coast occurred in reducing water with high concentrations of the competing ions Ca, Mg, Ba and Sr, and occasionally dissolved solids. The origin of the brackish water on the North Estonian coast has been under debate until the present. Reduced sulfate content and Ca-Na-Cl facies in groundwater may be related to the infiltration of saline water from the underlying crystalline basement [31]. The latest investigation of the wellfield intake of the Viimsi Peninsula revealed that groundwater chemistry changes (chloride content increased) over time in the Cm-V aquifer. The authors' opinion is that potential seawater intrusion could occur in the future [26].

2. Hydrogeological framework description of the Estonian homocline

The northern part of the Baltic Artesian Basin (BAB) fully covers the EH continental area and partially the offshore of the Gulf of Finland. The depth of the Cm-V aquifer along the coastline is 60–120 m from the surface. In the central part of Estonia, the depth increases to 250–300 m, and in the southern part up to 630 m. Most of the Cm-V aquifer groundwater belongs to the active exchange zone (shallow and partly intermediate depth), except the south region. The maximum thickness of the Cm-V aquifer system in Estonia is 80–90 m at the eastern part, diminishing to a few metres in the northwest [32, 33]. The Cm-V aquifer system overlays the Precambrian crystalline basement (granite and gneiss rocks). Granites of the Rapakivi are the most significant source of uranium-rich Precambrian basement rocks. The amount of Precambrian material also varies in moraine till at the coastal Klint lowland. These granites, which outcrop on the bottom of the Gulf of Finland and in southern Finland and Karelia, contain 3–10 ppm U, 10–50 ppm Th and 2.2–3.5% K [34]. In granites of northern Estonia, the maximum uranium content reaches 928 ppm and thorium 3215 ppm [35]. Uranium and thorium concentration ratio (U/Th) in basement rocks varies from 3.5 to 5. The upper part of the crystalline basement is a water-bearing permeable fracture porosity layer with a double porosity on the weathered surface sediments. Therefore, it could be considered as a lower part of the multilayered Cm-V aquifer system. The Cm-V aquifer system is presented by siltstones and sandstones and divided

into Voronka (V_2vr) and Gdov (V_2gd) aquifers. Geological cross-sections of the Cm-V aquifer system in the northeastern region are subdivided into two aquifers by the Kotlin clay formation (Fig. 1). Above lies the Lontova aquitard, which effectively protects territory from the leakage of O-Cm aquifer system groundwater and modern meteoric water percolation. In western Estonia, the Lontova aquitard facially changes to the water-bearing layer and forms a united groundwater body with the O-Cm aquifer system. The groundwater is perfectly protected from the above with S-O aquitard and Pleistocene tills. In the Upper Cambrian part of the O-Cm aquifer system, phosphorite is known as Obolus-sandstone (shelly phosphorite) of the Kallavere, Tsitre, Ülgase and Petseri Formations. The northernmost phosphorite deposits area is most enriched in U (~25–50 ppm) [36]. In the Lower Ordovician part of the O-Cm aquifer system, organic-rich marine metalliferous black shale, argillite rocks lie beneath most northern Estonia and western archipelagos. These rocks are characterized by high concentrations

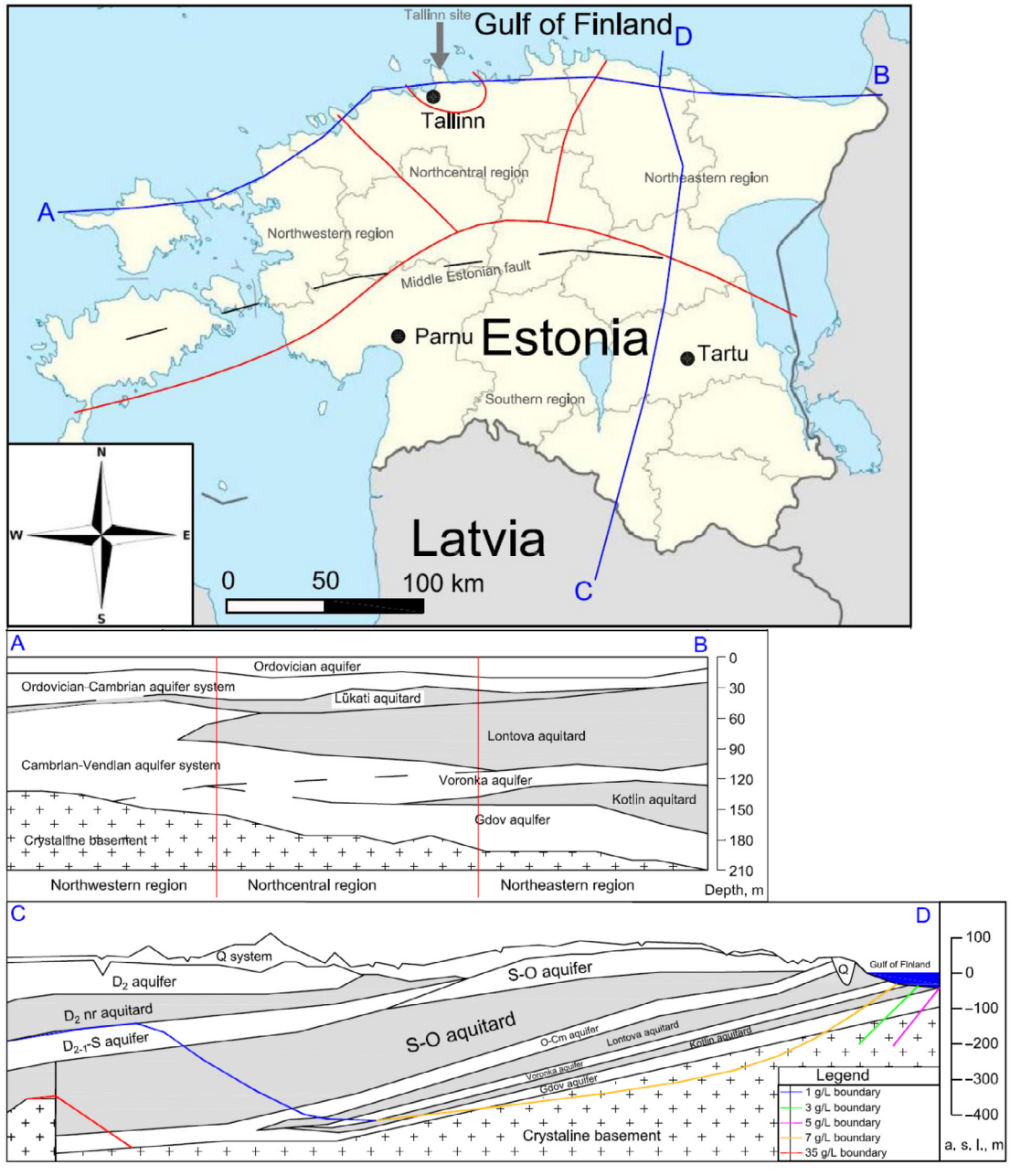

Fig. 1. Estonia map subdivided into isotope-hydrochemical regions (red lines): northwestern, northcentral, northeastern, southern and Tallinn site. Cross-sections: latitudinal A–B and longitudinal C–D.

of U (average 120 ppm). Thorium concentrations are analyzed in less than 100 drill cores, where the average varies between 13–17 ppm [35, 36].

In this study, all isotope-geochemistry data of groundwater is divided based on the region: Tallinn, northwestern, northcentral, northeastern and southern parts (Fig. 1). This division is based on the structural and hydrogeological setting – stratigraphic layer occurrence, framework (overlaying aquitard confining properties) and basement structural features. Middle Estonia Fault separates the southern part of Estonia. Most of the confining layer is absent in northwestern Estonia, allowing hydraulic connection between the Cm-V and O-Cm aquifer systems. The modern meteoric and Tallinn Bay seawater percolation into the Cm-V aquifer distorts isotope-geochemistry in the vicinity of buried valleys [18, 37]. The insertion of meteoric water into the Cm-V aquifer enriches residual groundwater with stable isotopes (δ^{18}O and δ^{2}H), dilutes dissolved solids content and alters a chemical type by binary mixing [19, 22–24, 26, 38].

The highest ^{226}Ra concentrations in the Cm-V aquifer system are near the coastal area [39]. A high radium content in the Cm-V aquifers may be due to its prolonged contact with the quite radioactive crystalline rocks of the basement, the reducing conditions of the aquifer (elevated radium solubility) and the presence of smectite–illite clays, in which a mechanism of absorption–desorption of radium can take place [40].

3. Methods and materials

Database of the Department of Hydrogeology and Engineering Geology of Vilnius University (DHVU) is a synthesis of long-term collaboration between laboratories and was developed since 1976 up to 2000 by the Lithuanian Geological Institute, and continued until now at the Vilnius University with the cooperation of Estonian Geological Survey, Institute of Geology of the Taltech University and from the published papers which include chemical and isotopic data from BAB [17–19, 40–45].

All these samples were analyzed for major ions and stable isotope δ^{18}O ratio expressed in the Vienna Standard Mean Oceanic Water (VSMOW) system. Depletion or enrichment in stable isotopes is based on the average annual value of δ^{18}O –10.4‰ in precipitation [46–48]. The summary of analyzed groundwater isotope-geochemistry data for the subdivided areas is shown in Table 1.

Table 1. The generalized main chemical and isotopic composition parameters of North Estonia groundwater samples.

		Depth, m	TDS, mg/L	Cl^-, mg/L	SO_4^{2-}, mg/L	HCO_3^-, mg/L	pH	δ^{18}O, ‰ VSMOW	SI calcite	SI halite
Northwestern region	MIN	40	118	9	1	73	7.6	–22.4	–0.2	–8.9
	AVG	185	706	270	17	164	8.1	–19.2	0.2	–6.7
	MAX	543	3889	2169	39	256	8.6	–11.5	1.1	–4.3
	STD	–	1013	616	12	50	0.2	2.2	0.3	1.0
Northcentral region	MIN	97	243	24	1	110	6.9	–22.0	–0.7	–8.0
	AVG	173	544	209	14	154	7.6	–20.9	–0.1	–6.5
	MAX	250	817	421	31	218	8.2	–19.5	0.4	–5.9
	STD	–	179	117	9	32	0.4	0.7	0.4	0.5
Northeastern region	MIN	101	153	6	0	91	7.1	–21.5	–0.8	–8.9
	AVG	205	721	295	3	190	7.8	–19.4	0.1	–6.0
	MAX	318	2025	1087	18	250	8.5	–12.0	0.6	–4.7
	STD	–	311	200	5	39	0.3	1.7	0.4	0.6
Tallinn site	MIN	60	226	10	0	42	7.0	–22.7	–0.9	–8.3
	AVG	132	583	213	12	176	7.8	–20.0	0.1	–6.6
	MAX	195	1260	629	56	366	8.6	–14.4	0.8	–5.5
	STD	–	265	163	15	57	0.4	2.7	0.4	0.7

Saturation indices (SI) for calcite and halite were calculated using the Phreeqc software database wateq4f. The following initial conditions were set (in cases this data was not measured): temperature 10°C, pe 0 and density 1 g/mL. A summary of Cl^-, SO_4^{2-}, HCO_3^-, pH, TDS, $\delta^{18}O$, saturation indices (SI) for calcite and halite is presented as maximum, average, minimum and standard deviation values in each region of north Estonia (Table 1). A selective Table 2 of North Estonia groundwater samples represents the main isotope-geochemistry data.

For the Tallinn intake, contents of ^{14}C were determined by counting liquid scintillation, stable isotopes $\delta^{18}O$ and $\delta^{2}H$ with mass spectrometers relative to VSMOW, $\delta^{13}C$ with a mass spectrometer according to the Pee Dee Belemnite (PDB) standard.

For Viimsi and Kopli peninsulas sites in the Tallinn intake and west Estonia islands groundwater, uranium content, and uranium isotope AR measurements were conducted at the Institute of Hydrogeology and Engineering Geology, Moscow [19]. The sampling volume was 200 L, from which uranium was concentrated on activated carbon in a special concentrator. The concentrator consists of a polyethylene case, cover for avoiding disturbance on a collection unit, a paper filter, a sieve for collection and a hose to release the collected water. Later on, uranium oxide was collected on a stainless steel foil via electrolytic precipitation. The prepared sample was analyzed using an α-spectrometer with a semiconducting detector, which enabled the determination of uranium isotopes (^{234}U and ^{238}U). Additionally, during

Table 2. The selective table of main isotope-geochemistry data of Estonia groundwater samples [45] and DHVU.

							Concentration units, mg/L							
Sample	Well No.	Depth, m	Zone	Index	pH	$\delta^{18}O$, ‰	Cl^-	SO_4^{2-}	HCO_3^-	Na^+	K^+	Mg^{2+}	Ca^{2+}	TDS
Tallinn, Viimsi	477	90	North, Tallinn	Cm-V	–	–22.7	351	26.5	159	130	13	20	109	809
Tallinn, Kopli	250	140		Cm-V	8.0	–21.6	521	34.4	165	210	11	32	121	1094
Tallinn, Kopli	14145	107		Cm-V	8.2	–21.5	403	3.7	156	137	11	26	114	851
Tallinn	815	–		Cm-V	7.9	–21.5	10	–	159	17	7	8	22	230
Tallinn	613	–		Cm-V	7.8	–21.5	629	36.6	152	208	10	41	162	1260
Karepa village	2517	121	Northeast	Cm-V	7.7	–21.5	140	0.2	210	92	8	12	41	504
Vinni village	2898	312		Cm-V	8.2	–20.1	207	0.0	167	112	10	18	49	563
Ahtme mining	2656	288		Cm-V	7.8	–18.4	738	2.0	91	372	12	25	50	1289
Narva-Joesuu city	2084	211		V2gd	8.5	–18.4	1087	3.2	170	684	10	22	49	2025
Kolga village	745	192		V-Cm	8.1	–12.0	6	3.3	110	7	–	4	22	153
Paldiski	Paldiski	140	Northcentral	Cm-V	–	–19.5	242	10.0	134	76	–	13	67	542
Laulasmaa village	584	159		Cm-V	8.0	–22.0	124	30.7	122	56	7	10	48	398
Kiiu village	1092	181		Cm-V	7.0	–21.4	336	10.2	171	93	10	27	107	754
Kehra city	1096	230		Cm-V	7.8	–20.7	421	0.5	156	108	9	27	96	817
Loksa city	680	145		Cm-V	7.2	–20.5	24	7.3	152	15	6	8	29	243
Dirhami port	2968	184	Northwest	Cm-V	8.2	–22.1	161	36.0	116	80	8	11	61	473
Hiiuma island, Nomme	13872	150		O-Cm	8.5	–11.5	9	3.8	73	5	1	4	22	118
Nissi commune, Turba	1576	110		O-Cm	8.0	–18.4	106	2.9	189	77	8	14	29	426
Kõrgessaare	13305	117		O-Cm	8.0	–20.6	78	25.9	159	59	7	10	28	323
Kuressaare**	10835	543		O-Cm	8.3	–17.6	2169	–	110	1040	24	68	477	3889

the analysis, the following parameters were determined: ratios of stable isotopes $\delta^{18}O$, $\delta^{2}H$ and $\delta^{13}C$ and concentrations of radiocarbon, tritium and uranium isotopes.

Uranium activity ratios of the Sosnovy Bor area of Leningrad District and Northern Dvina river delta site were published [49, 50] with the methodical reference [51]. The measurements of the $^{234}U/^{238}U$ activity ratio are made using mainly α-spectrometer or mass spectrometry techniques. Mass spectrometry (MS) used for uranium isotope determination are thermal ionization MS, inductively coupled plasma MS (ICP), ICP-MS with a multiple-collector option, etc. [52, 53]. The main advantages of mass spectrometry are faster analysis (minutes to few hours) and more accurate results, but the cost per sample is higher than alpha decay counting. The other important factor to consider is the bulk of the sample. Tens of millilitres are sufficient for mass spectrometry, while α-spectrometer requires a sample size from 10 to a few hundred litres. Specific preparation processes are required before the analysis as well. However, an α-spectrometer is still an abundant technique for uranium isotope AR determination when longer counting times and less accuracy are acceptable. In our study, we compare the results from older [19, 54] to more recent [49, 50] publications. In both cases, the α-spectrometer technique is used for analysis. The advances in sample preparation and concentration enable measuring the same uranium parameters with less sample size in recent research. The precision of alpha counting spectrometry is 2–10% (2σ) [52, 53]. Accounting for systematic and statistical errors may increase uncertainty up to 10–15% [19, 51]. This uncertainty is entirely acceptable in our study because results differ in the order of magnitude, and such errors do not change the fact that a significant anomaly of high AR exists.

For analyzing the evolution of $^{234}U/^{238}U$ isotope activity ratio in the studied aquifer systems, we used coupled independent models based on the determination in borehole water samples for AR and adjusted radiocarbon and ^{4}He ages. The use of uranium isotopes for the estimation of groundwater residence time is complicated because of the unknown initial activity ratio. North Estonian coast and Peipus Lowland and groundwater residence times were studied in 1975–1976 by radiocarbon dating techniques with initial chemical preparation and synthesis by benzene. At the same time, the helium gas concentration of borehole samples were analyzed using an INGEM-1 device at the Lithuanian Geological Institute [20].

4. Results and discussion

4.1. A new reality for talik system existence by $^{234}U/^{238}U$ activity ratio analysis

As mentioned previously, one of long-standing positions suggests that isotope-geochemistry anomaly formation on EH groundwater developed in paleo permafrost conditions. It was confirmed by the non-equilibrium fractionation model for stable environmental isotopes and chemistry [17, 18]. Besides, the high uranium isotope $^{234}U/^{238}U$ activity ratio, in principle, confirms permafrost existence [19]. The third proof of this hypothesis may be due to the display of high values of helium-4 concentration in groundwater [55, 56]. Because alpha particles are ^{4}He isotope nuclei, the phenomenon is related to U and Th geochemical anomalies. High helium content sites in Estonian groundwater directly connect with the radioactive decay in the Cm-V aquifer systems rocks. The α-recoil of ^{238}U balances the uranium decay series by daughter products: ^{234}U and ^{226}Ra to ^{234}Th and ^{234}U to ^{230}Th. The uranium decay is limited by secular equilibrium. Decay products and their parent isotopes represent a steady-state equilibrium, where the decay constants define the maximum possible intermediate daughter activity [57]. ^{234}U occurs due to the decay series of ^{238}U via ^{234}Th, therefore, the activity ratio of uranium isotopes ($AR = a^{234}U/a^{238}U$) forms a secular equilibrium in mineral and groundwater close to one. However, the studies revealed that uranium isotopes AR in groundwater also occur in a disequilibrium state because the mineral surface is in reality damaged or influenced by weathering processes of rock [52, 58–60]. Surface water mostly has AR ranging 1–2 [52, 61] and oceanic water 1.15 [52, 62, 63]. Deviations of the activity ratio from the secular equilibrium in groundwater are usually above 1 (often up to 2–3 and in exclusive cases >10). In general, there are two types of isotopic AR abundance variations: 1) it arises due to the α-recoil of the daughter ^{234}U isotope from the parent ^{238}U and 2) by preferential leaching from weathered rocks under oxidizing conditions in recharge

sites by meteoric water. In the oxidizing environment, a hexavalent uranium form has higher solubility, and groundwater can form enhanced AR if the down-gradient flow has difficulties discharging. Therefore, such phenomena significantly depend on the changes in thermodynamic conditions on redox boundary in aquifers. At greater depths, quadrivalent uranium species dominate, ^{234}U leaching is depleted and uranium may precipitate. Mainly ^{234}Th isotope recoil can produce ^{234}U atoms [2]. The ^{234}U isotopes are more mobile during the weathering of host rocks and can be leached into the water phase more efficiently than their parent nuclide ^{238}U. Change of oxidizing conditions to reduced during the down-gradient flow of groundwater from the redox front results in the secondary precipitation of uranium into the aquifer matrix and groundwater depletion of ^{238}U. Thus, AR in the groundwater increases [58, 64–66].

The 'α-recoil – weathering' model requires an additional consideration of mixing processes (mainly on the local sites for down-flow by leakage through aquitards) and the development of the Rayleigh progressive partitioning model for the permafrost condition. It is possible that in permafrost conditions the ^{238}U (as a heavier by atomic weight uranium isotope) could preferentially precipitate with carbonates during the reduction of U(VI) to U(IV) into an aquifer. In the partitioned residual groundwater, the accumulation of ^{234}U isotope occurs. The experimental studies of uranium isotopic fractionation in the formation of ice crystals at the partial freezing of trapped fluid were carried out in the Federal Center for Integrated Arctic Research, Russian Academy of Sciences [67].

The studies show that the forming ice is depleted by ^{234}U, and the residual part of water is enriched by radiogenic uranium atoms. A parent nuclide ^{238}U and a daughter product ^{234}U, connected by a single decay chain, in the solid phase formation behave differently, which confirms the existence of uranium in water in two forms: dissolved uranium in a form of individual compounds and uranium, which is in a mineral particle separated by the recoil nucleus ^{234}Th from the rock at entering the water. Thus, ^{234}U/^{238}U AR values in forming ice and residual water differ. The volume of unfrozen subpermafrost residual water becomes enriched with the isotope ^{234}U by saturation on the dispersed solid particles and in total uranium relative to the values of the original sample. The forming ice, in turn, is depleted in radiogenic ^{234}U atoms and total uranium. As shown by the freezing tests for borehole groundwater AR, the initial value of 5.89±0.02 was depleted for ice to 4.29±0.08 and enhanced for residual water to 5.99±0.02 [67]. In a regional conceptual model, most of the melted groundwater could be discharged during the permafrost thawing compared to a deep groundwater stagnant flow regime. A similar fractionation mechanism in paleo permafrost groundwater developed in the Estonian Cm-V and O-Cm aquifer systems for groundwater stable oxygen and deuterium isotopes.

In principle, an analogical chemical and isotopic distillation model for primordial uranium isotopes reduction proved in sandstone-hosted U ores, and the laboratory experiments suggest that ^{238}U is removed from the solution preferentially compared to ^{235}U during the partial reduction of U(VI) to U(IV) into minerals such as uraninite [68].

The uranium content in groundwater may vary from 10–6 to 1 ppm [52]. Usually, a higher uranium content corresponds to lower AR values. Due to the valence of uranium species in the oxidizing environments, U content is 1 ppb, and in the reducing ones it is 0.06 ppb [52, 69, 70]. In Sweden, at Stripa site natural uranium in the crystalline basement shallow groundwater is strongly oxidized, and waters have U contents of up to 90 ppb. In a deeper zone, the U content decreases below 1 ppb because of changing redox conditions into reducing. The intermediate-deep groundwater type is Na-Ca-Cl with saturated calcium content, depleted bicarbonates and high pH. Stable δ^{18}O and δ^{2}H values are depleted compared to modern shallow groundwater. The uranium isotopes AR value in the deep groundwater increases up to 7–10, related to long residence times (25–30 ka) estimated by radiocarbon dating 71]. However, AR change is strongly influenced by the U distribution within fractures, the extent of the rock–water interface, and the amount of ^{238}U in the solution. Dissolved radiogenic ^{4}He in the groundwaters increases with their depth of origin and depends on the U content of the granite and its fracture porosity [71].

The groundwater in Kopli and Viimsi Peninsulas during the periglacial infiltration of paleo-meteoric water, in oxidizing conditions, may have produced AR up to 25–40. As a result, the uranium content formed in the range 0.05–0.25 ppb. Such an amount

of ^{238}U is closer to the values found in the reducing groundwater environment. It indicates that high AR values are related to a long groundwater residence time due to the ^{234}Th-recoil release of ^{234}U. In permafrost, a significant part of α-recoils ^{234}U was sealed beneath underground ice and after the thawing of the permafrost layer caused an excessive ^{234}U content in the aquifer system. After the Ice Sheet retreat, the groundwater in the studied aquifer system was predominant in the reducing conditions. Modern-meteoric water recharge was absent, except in places near the slopes of the buried valley on the northern coast of the Gulf of Finland. Due to periodic climate changes during the Pleistocene, the secondary quadrivalent uranium precipitation could occur multiple times are changed the redox barriers at glacial-interglacial boundaries. In the northwestern part of Estonia, the same oxidizing process could occur through a deep-set talik system, which continues to the south. Since the end of cryogenic processes, the formation of uranium isotope AR anomaly in the entirely reducing condition began.

The isotopic δ^{18}O content of groundwater shows that continuous permafrost existed on the BAB territory with a local open talik net during the Late Pleistocene. The conceptual talik location scheme was reconstructed in a northern part of the BAB, which does not disturb a general opinion about the isotope-geochemistry features (Fig. 2). The talik system framework was grounded on the seabed and onshore lowlands, where significant erosion occurred. The bathymetry revealed the main lineament zones and eroded sites: Gulf of Finland, North-Central Baltic Proper, Gulf of Riga, Liivi Lowland and Alutaguse-Peipus Lake Lowland. Southwards of Peipus Lake, to Russian territory, talik is connected with the Pskov buried valley lowland. The general branches of the talik system could induce lateral flow under sub-permafrost aquifers and vertical discharge zones. The groundwater flow from the sub-permafrosted zone upwards is limited by regional Kotlin and Lontova aquitards and permafrost terrains slabs, which may locally occur in discontinuous permafrost sites.

The proposed talik system theory may explain various isotopic-geochemistry and chemical types distributed in groundwater of the O-Cm and Cm-V aquifer systems. Aquifer recharge with precipitation and surface water can occur from lakes and rivers near the talik location. Flow paths may as well connect in uplands through supra- and intra-permafrost units (Figs 2, 3).

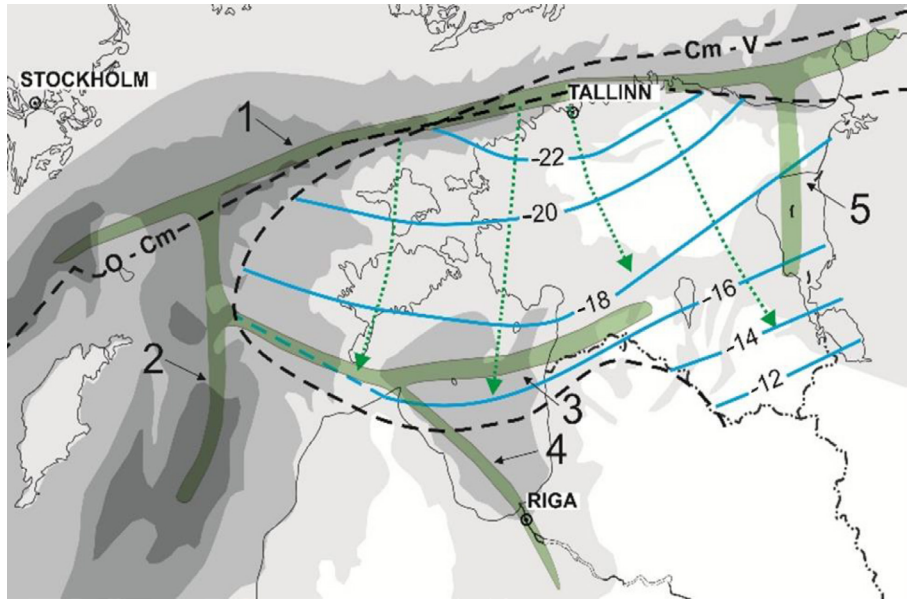

Fig. 2. Talik zones reconstruction scheme for the Pleistocene time on the northern part of BAB. Numbers of taliks on the scheme: 1) Gulf of Finland Talik, 2) North–Central Baltic Proper Talik, 3) Liivi Bay Northern Talik, 4) Liivi Bay Southern Talik, 5) Alutaguse-Peipus Talik. Blue lines represent a stable isotope ratio δ^{18}O (‰) in the O-Cm-V-B unit groundwater. Green arrows represent lateral flow in sub-permafrost aquifers.

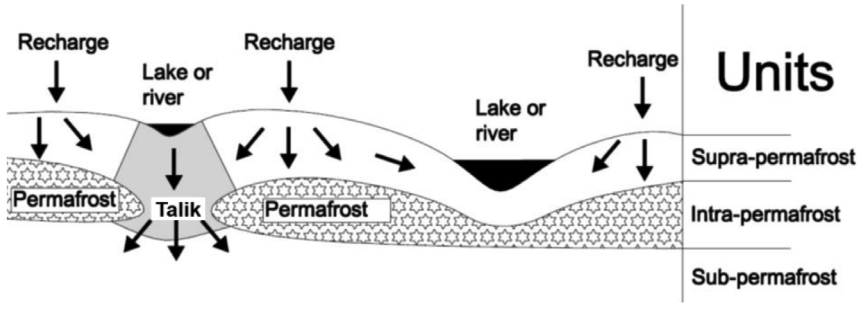

Fig. 3. Principal cross-section schemes of Talik zones from after [72, 73].

A strongly depleted $\delta^{18}O$ content is observed in the north Tallinn zone, where its values are down to –22.5‰ (Tables 1, 2). It is noteworthy that a depleted $\delta^{18}O$ isotopic composition in the Tallinn intake (Kopli and Viimsi Peninsulas) sites is inherent with high uranium isotope ratios and formed by permafrost conditions [18, 19].

In the Cm-V aquifer system hydraulically connected with the underlaying basement, processes in a frozen underground state took place for a long time. The prolonged existence of permafrost in a frozen underground state probably caused the accumulation of ^{234}U isotope in a solution like a daughter product of the ^{238}U from the disturbed crystal lattices of minerals [19]. As a result of permafrost degradation, a quick filling of the aquifer with surface waters and the entrance of accumulated ^{234}U from the crystal lattices of minerals into an aqueous phase occur. It is possible that in northwest Estonia, an additional superposed inflow with the groundwater having extremely high AR values leaked from an alum-shale layer (O-Cm) of the sub-permafrosted part. Obviously, the intrusion of the Last Glacial Maximum (LGM) ice sheet meltwater into aquifers cannot result in a high $^{234}U/^{238}U$ isotopic activity ratio. Some authors suggested that the Pleistocene ice sheet meltwater intruded into an aquifer can exchange reduced environment to oxidizing [74].

Äspo sites in Sweden present an excellent illustration of a similar situation [75]. Authors discuss that in reducing conditions, the quadrivalent ^{234}U is leached in preference to ^{238}U, resulting in the rock matrix obtaining a negative shift of uranium activities ratios [75]. This shift is the precondition to the high solubility of ^{234}U, situated in mineral crystal lattices (produced by uranium and ^{234}Th from fracture surfaces into solution), resulting in groundwater with elevated AR. For the Laurentide Ice Sheet retreat, the ice meltwater inflow rate promotes the (AR) results in a secular equilibrium state near 1 [76].

In the eastern part of the Gulf of Finland within the Baltic-Ladoga lowland segment (area of the Luga Bay, the Koporye Bay and Saint Petersburg), the substrate is mainly composed of the Upper Vendian–Lower Cambrian impermeable clays, siltstones and sandstones. Valleys are V-shaped, widths of 800–3000 m, depths down to 90–110 m b.s.l. cut in the pre-Quaternary bedrock 50–80 m. Near the Koporye Bay coast site for Sosnovyi Bor (Leningrad District, Russia) wellfield, the $^{234}U/^{238}U$ ratio of Lontova clays is 0.85, in the weathered core of basement rocks it is 0.75. The uranium isotope ratio of the Cm-V aquifer paleogroundwater varies from 0.48 to 0.65 (Table 3) [54]. The modern meteoric recharge increases uranium ratio up to 1.1 due to oxidation conditions (buried valleys and outcrops sites). Most likely, in the vicinity of Koporye Bay (Cm-V outcrop), near the former periglacial talik, an active infiltration recharge existed. Uranium-234 was intensively leached during the Pleistocene time and removed from the aquifer system by discharge flow to the surface water body. Leaching occurred from low U-Th content host rocks by recharge–discharge flow interaction either sub-, supra-permafrost aquifer or surface waters. Koporye Bay talik could have been connected as a branch to the main talik of the Gulf of Finland (Fig. 2). On the contrary, the Cm-V aquifer system is isolated only by the Kotlin aquitard in northern Estonia because the Lontova Blue clay offshore is absent. So, we may conclude that low $^{234}U/^{238}U$ ratios in the Sosnovyi Bor are caused by long-term active dissolving of uranium from the host rocks where the uranium content is low.

Table 3. Isotopes and chemistry of the Tallinn and Sosnovyi Bor intake for the Cm-V aquifer system. Modified after [18, 19, 49, 50, 54].

Well No.	TDS, g/L	$\delta^{18}O$, ‰	$\delta^{2}H$, ‰	$\delta^{13}C$, ‰ PDB	$^{234}U/^{238}U$, (AR)	^{14}C, pmC	Adjusted ^{14}C and uranium decay ages, ka	Depth, m b.s.l.
Kopli Peninsula								
14	0.95	–19.4	–150	–15.0	8.0	9.4	18.4	100–125
22	0.92	–20.6	–156	–16.2	3.3	16.8	15.4	50–120
17	0.43	–15.2	–110	–15.0	5.1	24.0	11.8	115–130
18	0.42	–15.1	–111	–12.5	3.0	43.0	5.5	116–135
19	0.44	–21.1	–160	–16.2	16.0	7.8	21.7	112–136
20	0.43	–21.3	–165	–16.2	26.0	7.1	22.5	90–140
Viimsi Peninsula								
21	0.46	–21.5	–160	–15.0	4.0	16.7	14.8	45–115
27	0.84	–22.5	–170	–12.4	15.1	33.6	7.5	60–125
26	0.35	–12.0	–90	–12.6	2.7	54.7	3.6	80–122
25	0.53	–14.4	–105	–13.4	11.5	53.2	4.3	60–110
66	0.7	–15.0	–111	–11.2	–	48.1	3.7	59–125
67	0.8	–16.3	–125	–14.7	–	39.2	7.6	56–120
1A	9.3	–11.6	–	–	–	–	–	110–120
Sosnovyi Bor site								
P9	1.5	–15.5	–	–	1.1	–	5.5	–
P6	–	–12.6	–86	–	0.63	–	–	180
P14	2.4	–18.8	–	–	–	–	9.0	160
П4	2.7	–15.7	–108	–	0.48	–	–	191
П2	2.9	–13	–98	–	0.64	–	13.0	240
Northern Dvina river delta site								
8mz	22.25	–12.2**	–94.4**	–	2.97	–	460*	120
La5	15.7			–	6.19	–	110*	200
No1	8.9	–7.7**	–58.3**	–	6.72	–	80*	90
Mi	5.3	–14**	–107**	–14.6	7.16	1.7	33.0	150–201
B1	9.14			–15.6	5.41	5.79	26.1	105
Lo	0.79	–13.8**	–100**	–11.2	5.94	37.03	5.4	80
W6	0.732			–9.6	2.86	25.3	4.0	80–90
3e	0.138			–12.3	2.26	34.18	2.1	20–25

Note: borehole 1A is located on the Aegna Island (Tallinn Bay offsore); Sosnovyi Bor site is located on the eastern coast of Koporye Bay (Leningrad District); * uranium (^{234}U–^{238}U) isotopic dating of age; ** the average value of $\delta^{18}O$ and $\delta^{2}H$ stable isotopes.

A very high $^{234}U/^{238}U$ ratio (<20) is fixed in the groundwater near the Arkhangelskaya kimberlite pipe space at the M.V. Lomonosov deposit on the White Sea coast. The Vendian rocks are characterized by elevated or anomalous U, Th and K contents concerning the background values. This halo of non-equilibrium uranium is localized in the near-pipe space and revealed in Vendian aquifer system rocks consisting of siltstone and sandstone and rocks of the epiclastic unit in the pipe at the contact with host rocks [77]. The authors explained the deviation of the isotopic equilibrium of uranium by the dynamics and long-term circulation of underground water along the tectonic fractures bounding the pipes.

The distribution of radioactive isotopes in the Vendian aquifer system is well studied in the Northern Dvina River delta (NDB) at the Arkhangelsk–Severodvinsk–Novodvinsk site [49]. The study area is presented by non-continuous permafrost, which is confined by peat soils up to 15 m. The average annual temperature in this territory is –0.5 – –1.0°C. Here the Vendian aquifer system and intermediate deep old brackish groundwater of Vendian Mezen aquifer inversely discharge to the above layered fresh Vendian Padun aquifer, which is recharging by modern meteoric precipitation. The maximum (AR) values of Vendian aquifers groundwater in deeper, reducing zone are 4.8–7.2 and the adjusted ^{14}C age range is 17–33 ka. Brackish groundwater is more depleted with $\delta^{13}C$ and $\delta^{18}O$ contents –15.5 to –16.6‰ and –14.4‰, respectively, TDS values between 4.3 to 9 g/L. In the oxidizing recharge zone freshwater, $\delta^{13}C$ and $\delta^{18}O$ contents are –11.7‰ and –13.8‰, respectively. The fresh groundwater residence time is estimated from 0.3 to 16.4 ka. The medium AR (1.3–5.9, average 3.0) is characteristic of this water. Near the redox barrier, old saltwater has ages ranging from 17 to 33 ka with TDS from 4 to 13 g/L and high AR (4.8–7.2, average 5.9). Below the redox barrier, in reduced lenses at the buried paleo-valley bottom, the elevated concentrations of uranium are preserved. The precipitated U(IV) uranium concentration in rocks reaches 20 ppm, and AR in rocks decreases to 0.5–0.9. But, complete precipitation does not occur because recoil continues, and both uranium isotopes enter the water. In these areas, the most dangerous aspect is the flow of groundwater from the underlying horizons, since during the operation of water supply wells it can lead to the creation of local zones of oxidizing conditions in the perforated boreholes screen zone and the transition of uranium into a solution [49].

Cyclical glaciations and marine transgressions strongly influenced the geochemical evolution of groundwater systems of the Arkhangelsk region. In the lower part of the Vendian Mezen aquifer, brines are found at >1 km depth. Near the modern sea coast, shallow groundwater is enriched by heavy stable isotopes, average values $\delta^{18}O$ = –7.7‰ and $\delta^{2}H$ = –98.9‰ [50].

We made the correction of the ^{14}C ages of the groundwater at the Tallinn intake using Eq. (1), based on the background value of $\delta^{13}C$ = –15.0‰ PDB used in [78], where $\delta^{13}C$ and ^{14}C are in per mil and pmC in the groundwater sample, respectively:

$$t = 8267 \times \ln(-6.7 \times \delta^{13}C/^{14}C). \quad (1)$$

At the Tallinn intake, the Cm-V aquifer system groundwater $^{234}U/^{238}U$ AR varies from 3.6 up to 26 at the 50–140 m depth range (Table 3). The increase of uranium AR slightly corresponds to TDS elevation from 0.35 up to 0.95 g/L. In Holocene, strongly reducing conditions prevail in the Cm-V aquifer, with oxidation–reduction potential Eh varying from –150 to –250 mV. Redox environment transition to oxidizing mainly appears near buried valleys and Eh values vary from –50 to +100 mV [40].

Enhanced accumulation of a more soluble uranium-234 isotope and high $^{234}U/^{238}U$ AR formation could begin in the periglacial period before LGM. The drop in the sea level opened a highly elevated cliff in the Estonian western and northern parts. Steep (150 m amplitude elevation) landscape could be formed toward the eroded seabed of the North-Central Baltic Proper and the Gulf of Finland valleys. Connected lake and river systems established a new recharge/discharge boundary for periglacial groundwater flow. A redox front separated above (near-surface) layered oxidized zone in the northwest to north-east part from the deeper aquifer part with reducing conditions in the south-eastern direction. In deeper parts (300–500 m), oxidation environment might be possible only by mixing supra- and sub-permafrost aquifers groundwater in open Liivi Bay (Gulf of Riga) and Alutaguse-Peipus talik systems. It probably caused a prolonged (10–20 ka) enhanced accumulation of the ^{234}U atoms in the sub-permafrosted aquifer due to α-recoil from parent ^{238}U aquifer rocks in leaching or damaged crystal lattices of U-Th rich minerals. Later on, groundwater with high (AR) values was moved toward the discharge sites with a reduced decay regime. A natural process on the periglacial reduced Eh conditions occurred for a long time leading to the dis-equilibrium of $^{234}U/^{238}U$ (AR $\gg$ 1) in the groundwater of the O-Cm and Cm-V aquifers (Figs 4, 5).

For example, the maximal AR values 40–56 are observed on the Saaremaa Island and Viimsi Peninsula [19]. The latest publications indicate that in southern Finland, the Middle Weichselian glaciation and the interstadial did not occur

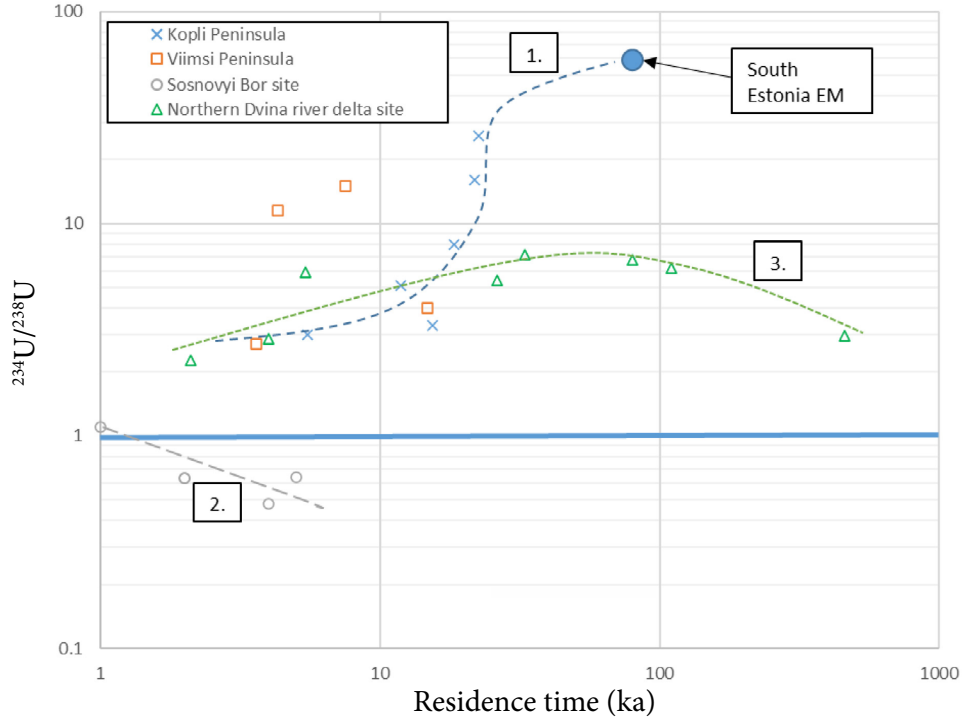

Fig. 4. Residence time and $^{234}U/^{238}U$ activity ratio diagram. 1. Tallinn intake. 2. Sosnovyi Bor intake. 3. Northern Dvina site.

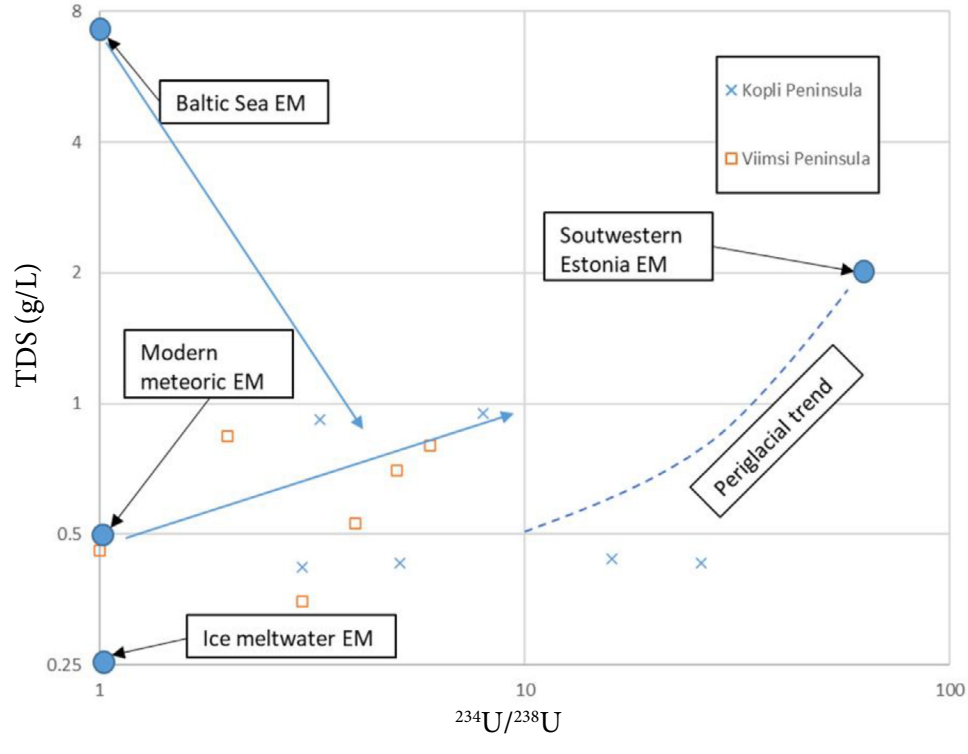

Fig. 5. TDS and $^{234}U/^{238}U$ activity ratio diagram in Tallinn intake.

[79]. The Late Weichselian glaciation Marine isotope stages (MIS2, 29–11 ka ago) were preceded by a nearly 90 ka long, poorly known non-glacial period, featuring tundra climate with permafrost. A new Middle Weichselian paleoenvironmental scenario had much longer periglacial conditions

before LGM in Finland, indicating that permafrost could have easily penetrated >450 metres depth b.s.l. [79]. Therefore, the single LGM glaciation evidence during the Weichselian time in the EH is substantial [80].

Helium ages reveal that south Estonia groundwater may originate in the Middle Weichselian periglacial time. The evaluation of the southern part of Alutaguse-Peipus Talik, Värska site, for O-Cm (depth 463 m) and Cm-V (545 m) aquifer system groundwater radiogenic ^{4}He ages are 81 and 86 ka (MIS5 a-b substages), respectively. Groundwater at the Häädemeeste site close to the Liivi Bay Northern talik (depth 610 m) ^{4}He age is 150 ka corresponding to the Middle Pleistocene Saalian Glaciation by MIS6 [81]. In eastern Estonia, the middle part of Alutaguse-Peipus Talik (Alatskivi borehole) ^{14}C adjusted age is younger (26.8 ka) compared to the Tapa well on the Pandivere Highland northern (33.1 ka) [18]. In the depth of 280 m Alatskivi groundwater, TDS is 1.5 g/L, while Tapa is 0.5 g/L in 242 m depth. Such difference could be caused by talik conditions, which promote the inversion. These ages support prolonged periglacial permafrost conditions on the EH (Last Glacial and Saalian times).

A good relationship between the ^{234}U and ^{4}He contents was explicitly demonstrated for Canada's periglacial conditions [76]. Freshwater is devoid of radiogenic ^{4}He, shows AR close to equilibrium (1), saline older groundwater contains higher ^{4}He content and increased AR up to 6 [76]. The authors suggested that opening new fractures in periglacial sites provided additional surfaces for host rocks, increasing ^{234}U and ^{4}He migration and escaping the water [76]. A similar process may occur on EH – high AR and ^{4}He contents anomalies are associated on the West Estonian Lowland, North Estonia coastal plain and Alutaguse-Peipus Lake Lowland. These areas are frames to the biggest taliks. The reality of open talik systems, which functioned as a redox barrier for radioactive elements transformation during the LGM, is evident. In a periglacial environment, the sub-permafrost O-Cm and Cm-V aquifer systems, and basement fractures zone were connected to a single hydraulically joint unit, where the groundwater was altered by series of isotope-geochemistry fractionation into a rare hydrogeologic body. The relationship of the ^{234}U and ^{4}He excess in the aquifer explains the existing redox boundary from the external sources of talik system between supra- and sub-permafrost units.

A reverse direction AR trendline appears at the sites with fully or partially cut aquitards near the coast (paleo valleys). Intense depletion of AR occurs due to meteoric precipitation at the onshore parts and the saline water intrusion from the seaside. These processes are confirmed by δ^{18}O and TDS in groundwater (Fig. 5 and Table 3). The TDS versus ^{234}U/^{238}U activity ratios analysis shows that a high uranium isotope activity ratio belongs to the groundwater of the Ca-Na-Cl-HCO_3 and Na-Ca-Cl-HCO_3 types. Between AR values 10–26, the groundwater salinity increases up to 0.43–0.84 and more g/L. The Na/Cl ions ratio for these chemistry types is very low (0.45–0.6) and shows a high groundwater metamorphism degree which evidences long residence times.

The influence of meteoric groundwater on groundwater near buried valleys using a stable isotope δ^{18}O ratio was proven in multiple studies [17, 19, 29, 32, 33, 82]. Modern groundwater tends to enrich the oxygen ratio isotopic values towards the average annual precipitation (–11.4 per mil). Pleistocene time groundwater is usually depleted (down to –23 per mil). The relation between uranium AR and oxygen-18 shows that modern groundwater is closer to the AR equilibrium, while Pleistocene age groundwater AR is significantly higher. In cases of modern and paleogroundwater mixing, the depletion of uranium AR values occurs. It could be described using end-members of this study from Viimsi and Kopli Peninsula. The borehole No. 26 AR 2.7 and δ^{18}O 12‰ represent groundwater with a higher portion of modern-meteoric water. In borehole No. 20, AR = 26 and δ^{18}O 21.3 ‰ indicate paleogroundwater. In places where strongly by stable isotopes depleted groundwater is observed, almost none of the meteoric water influence occur.

In the sites where the groundwater from the reducing zone is mixing from perched modern waters via buried valleys, the AR values are intensively lowered (Fig. 6). Evolution of the initial periglacial groundwater on northern Estonia developed by influence of LGM and Baltic Ice Lake meltwater, modern meteoric recharge and Baltic Sea intrusion. That is proved according to the depletion of AR values and also by ^{14}C data.

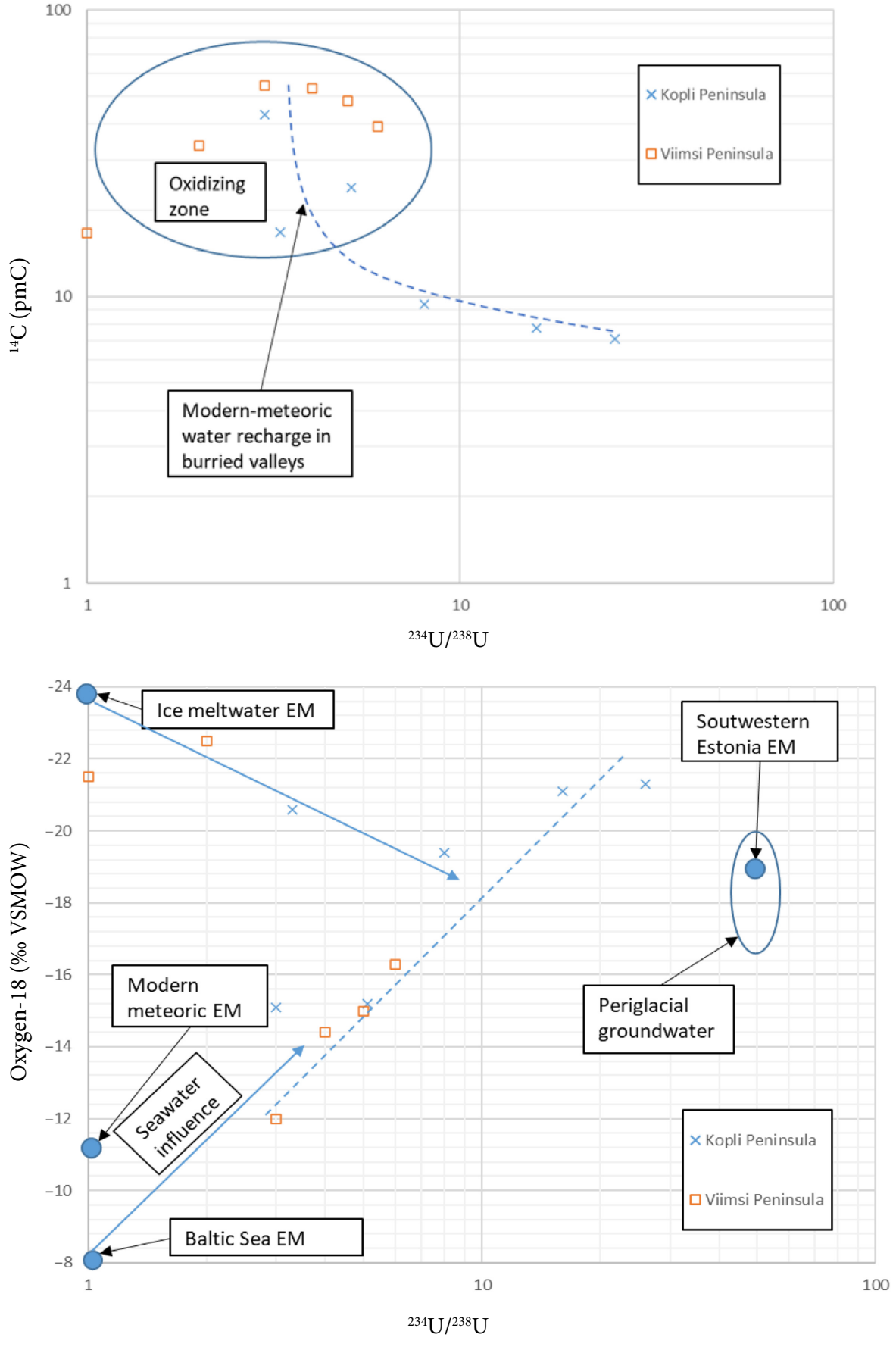

Fig. 6. ^{234}U/^{238}U activity ratio vs ^{14}C and δ^{18}O content diagrams.

LGM groundwater background parameters of the Tallinn intake are $\delta^{18}O$ –22.5‰, $\delta^{13}C$ –16‰ and TDS 0.35–04 g/L. The highest observed AR (26) in boreholes are distant from paleo valleys. Groundwater extraction caused background values to change, toward freshening, a drop of AR (down to 3.0), enrichment of $\delta^{18}O$‰ and $\delta^{13}C$‰ content to –12.0‰ and –12.4‰, respectively. Increased ^{14}C content is observed in these samples (up to 54.7 pmC) (Fig. 6). The sea intrusion results in elevated TDS up to 0.95 g/L groundwater, $\delta^{18}O$ may increase up to –19.4‰, $\delta^{13}C$ to –15‰ and ^{14}C to 16.8–33.6 pmC. Sea intrusion influence is observed in boreholes No. 14 and 22 at Kopli Peninsula and No. 27 at Viimsi Peninsula (Fig. 6, Table 3). Change in the chemical composition of this groundwater indicates a significant increase in TDS and SO_4/Cl ratio during 1977–1988 [17].

4.2. The cryogenic groundwater identification based on stable isotope-geochemistry

In a periglacial environment, groundwater flow and isotope-geochemistry zonation was strongly affected by cryogenesis in the O-Cm, Cm-V aquifers and basement fractures. Therefore, a hydraulically connected Lower Ordovician-Cambrian-Vendian-Basement groundwater (O-Cm-V-B) should be analyzed as a single unit. Generalized data provide the evidence that permafrost may strongly influence the groundwater composition (Table 1). Most samples show elevated pH values up to 8.6 (average 7.6–8.1). An increase in calcium, magnesium and bicarbonate content makes the water oversaturated with carbonate minerals (calcite and dolomite), resulting in their precipitation. The decrease of these ions follows the precipitation: north Estonia alkalinity content is down to 42 mg/L averaging between 154 and 190 mg/L (Table 1), similar to permafrost terrains in Yakutia, Russia [9, 10, 12]. The chloride content in the Cm-V aquifer groundwater average values is 209–295 mg/L, which may result from brine rejection in the relic residual water fraction. As mentioned before, seawater intrusion may also be the case during the interglacial time maritime conditions and present when seawater was mixed with in situ O-Cm-V-B unit groundwater.

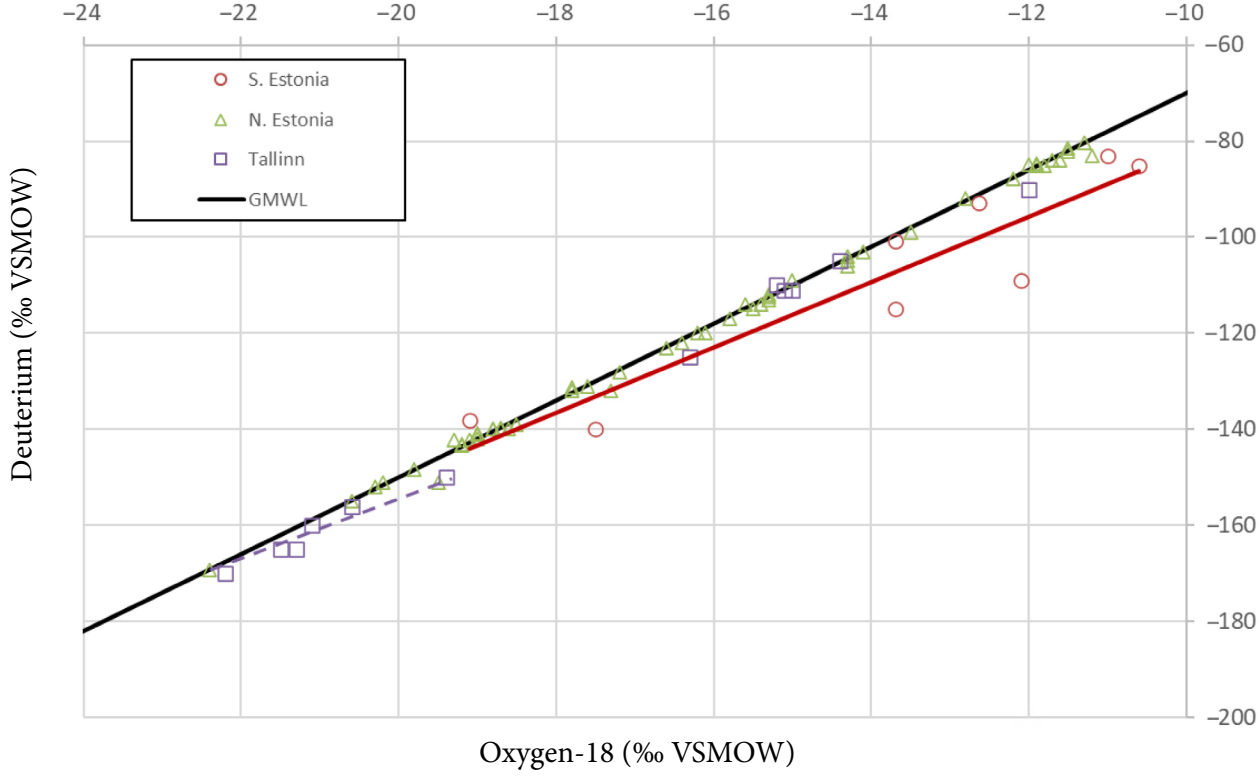

Fig. 7. Craig diagram of Estonia groundwater. A dashed line is the permafrost line in Tallinn and a red line is non-equilibrium snow meltwater or surface water percolation trend in the Pärnu site, close to the former southwestern Estonia talik system.

Two deviations from the GMVL are observed on the Craig diagram (Fig. 7) permafrost and snow meltwater. The northern part of Estonia Cm-V groundwater chemical facies varies mainly between Ca-Na-Cl, Ca-Na-Cl-HCO_3, and Na-Ca-HCO_3-Cl. Facies differences could be explained by hydrochemical stratification, which occurs during the cryogenic concentration. Assuming that the permafrost formation is a gradual and slow process, brine rejection and mineral precipitation should result in various groundwater types [9, 10, 17]. Groundwater in the upper part of the aquifer is fresh, Na-HCO_3-Cl type; deeper, the residual portion is mainly sodium chloride facies. Cryogenic groundwater from the Tallinn intake is Ca-Mg-Cl, Ca-Na-Cl, and Ca-Cl type. Exclusive Ca-Na-Cl type groundwater is found in the deepest BAB aquifers (>1.5 km depth) under stagnant conditions (Lithuania, Kaliningrad and Poland); therefore, it is highly unlikely that it could be the source of dissolved solids for the Cm-V aquifer system in northern Estonia. The northward migration of these deep brines is stopped by the uplifted horst barrier as the low permeability lineament zone of the Liepaja–Riga–Pskov. The northwestern part unit is subdivided into two bodies, the Cm-V and O-Cm aquifer systems, where Na-Ca-Cl-HCO_3 and Na-HCO_3-Cl facies are observed, respectively (Fig. 8). Different chemical types may evolve due to the cryogenic hydrochemical stratification mentioned before. In the (O-Cm-V-B) body, the overlaying O-Cm water was likely exposed to more cryogenesis cycles, resulting in multiple carbonate precipitation occasions and depletion of calcium and bicarbonate. The lower part (Cm-V) is also more depleted $\delta^{18}O$ (down to –22.5‰), compared to O-Cm (~–19‰), but more concentrated in TDS. The Rayleigh distillation trendline could easily explain this distribution towards depletion in the cases of residual water fraction F > 0.5 [2]. The same isotopic depletion scenario is applicable in other northern Estonia (O-Cm-V-B) groundwater as well. Northward from 1 g/L TDS boundary in the central part of Estonia, chemical and isotopic inversion occurs: $\delta^{18}O$ is depleted by 3‰, while chloride content rises to 3 and more g/L. Southwards from the freshwater boundary (1 g/L), $\delta^{18}O$ values are enriched by 6‰, Cl^- content increases to 10–12 g/L (Fig. 1).

The evolution of the cryogenic groundwater could be well established on Na/Cl and Br/Cl ratios diagram (Fig. 9) [15, 83, 84]. Groundwater of the O-Cm aquifer in the Br/Cl range 0.002–0.004 is a Na-HCO_3-Cl type, and the samples with the

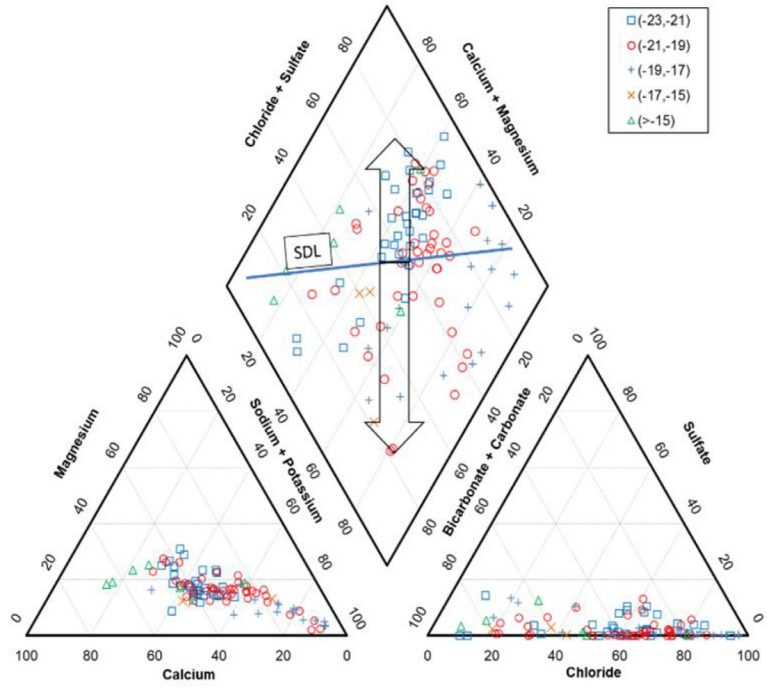

Fig. 8. Piper diagram of $\delta^{18}O$ based on groundwater chemistry. The line represents the seawater dilution line (SDL) and arrows show cryogenesis induced shift toward Na-HCO_3 and Ca-Cl corners.

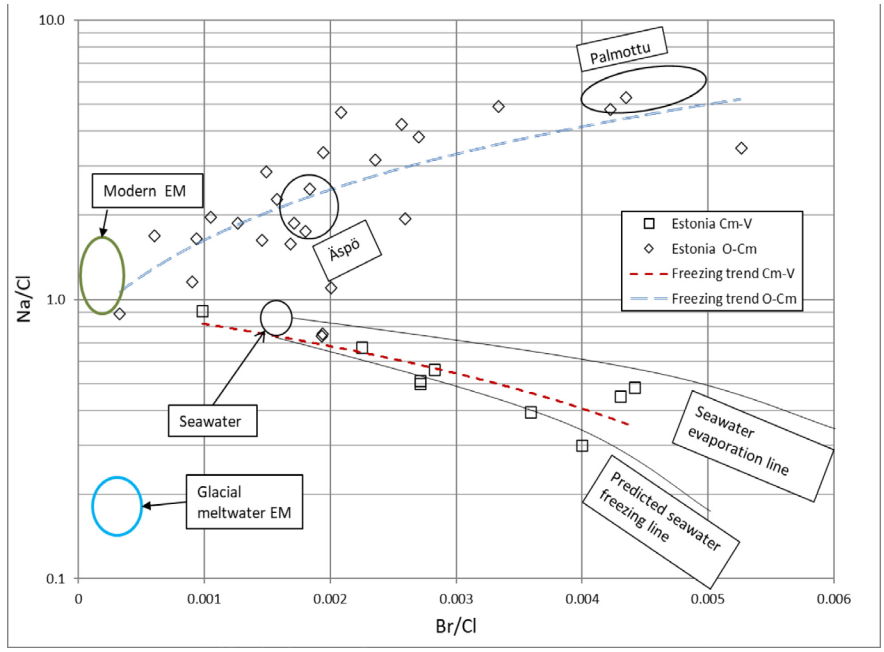

Fig. 9. Na/Cl and Br/Cl diagram of the northern Baltic region. Seawater evaporation [85] and predicted seawater freezing [84] trends are included as an example of water chemical alteration. Äspö and Palmottu groundwater is added to reflect the cryogenic effect in the Fennoscandian Shield [83]. The groundwater of EH is divided into the Cm-V and O-Cm aquifers (where bromide data was available).

ratio >0.004 are Na-HCO_3. This groundwater $\delta^{18}O$ content varies between –19.0 and –18.5‰. Chemical type transformation is due to carbonate precipitation, calcium, magnesium and partly bicarbonate being removed from the solute. Ca-dominated initial water (before freezing) could have resulted in Na-HCO_3 diverse water facies and manifest in the O-Cm freezing trend. The evolution of the O-Cm groundwater composition coincides with the data from Scandinavian Shield, Äspö and Palmottu sites [83].

The Cm-V aquifer groundwater seems to be altered by increasing Br/Cl and a substantial decrease of Na/Cl ratios, following seawater freezing and evaporation trends. Groundwater with Br/Cl values over 0.004 is Ca-Na-Cl type $\delta^{18}O$ values varying from –21.5 to –20.7‰. The evaporation process, which occurred in the deep BAB groundwater formation [37], is unlikely to be the case in the Cm-V aquifer groundwater alteration because it evolved during the Pleistocene when the climate was cold, causing periglacial permafrost formation. The evaporation should have enriched $\delta^{18}O$ values, while data shows the opposite. The predicted freezing trend of the Cm-V groundwater could result from the wasted bicarbonate content in calcite precipitation. The initial water, in this case, should have been less Ca-dominated and more saline, compared to the O-Cm. The rejection of dissolved solids increases calcium, sodium and chloride content in residual fluid, but due to lack of bicarbonate, further mineral precipitation does not occur; the solute concentration may develop without disruptions. Such a process could lead to the formation of Cl-HCO_3-Ca-Na chemical type groundwater and explain the palaeo-freezing trend of the Cm-V, O-Cm aquifer systems and in the crystalline basement water through permafrost (Fig. 9).

5. Conclusions

General three end-members (glacial meltwater, seawater and modern mixing model) cannot explain the diverse origin of the northern part Baltic region groundwater. The fourth, periglacial cryogenic process, end-member, is introduced to evaluate its role in the paleogroundwater origin. $^{234}U/^{238}U$ activity data calibration with radiocarbon and ^{4}He ages proves that old paleogroundwater was formed due to the talik system development in the permafrost

environment. The isotope-geochemistry content of the north Baltic region groundwater has been affected by the permafrost during the Last Glacial Maximum, Middle Weichselian and Saalian Glaciation when taliks existed.

Paleogroundwater recharge could occur near lakes and rivers underlined by talik, adjacent permafrost-free covered uplands, or through supra- and sub-permafrost connections. These circumstances, in general, altered the chemical and stable isotope composition of groundwater. Permafrost formation is followed by brackish rejection and Rayleigh distillation in groundwater with secondary processes such as carbonate and sulfate mineral saturation and precipitation leading to the change of chemical facies. These processes are observed in the present permafrost terrain ground ice and groundwater, primarily increased pH, lower bicarbonate content, elevated sodium and chloride concentration. Anomalous isotope-hydrogeochemistry features of the O-Cm and Cm-V and basement groundwater led to forming a joint hydrogeological unit (O-Cm-V-B) which is presented by anomalously high $^{234}U/^{238}U$ ratio values in the reducing environment during long residence time by superposition of the uranium decay products accumulation and distribution features from that groundwater body host rocks.

The freezing of groundwater formed the residual part below the underground ice with depleted stable isotopes and increased TDS. This groundwater up till the present is being affected by meteoric water and seawater locally via paleo valleys. A regional review of the sedimentary cover groundwater and salinization by Ca-Cl type water from the crystalline basement layer at the Tallinn wellfield proved the cryogenic origin of groundwater based on Br/Cl and Na/Cl trends revealing its distinct origin in the context of the BAB groundwater framework.

References

[1] M. Lehmann and U. Siegenthaler, Equilibrium oxygen- and hydrogen-isotope fractionation between ice and water, J. Glaciol. **37**(125), 23–26 (1991), https://doi.org/10.3189/S0022143000042751

[2] I. Clark and P. Fritz, *Environmental Isotopes in Hydrogeology* (Lewis Publishers, Boca Raton, 1997)p.28,https://doi.org/10.1201/9781482242911

[3] J.R. O'Neil, Hydrogen and oxygen isotope fractionation between ice and water, J. Phys. Chem. **72**(10), 3683–3684 (1968), https://doi.org/10.1021/j100856a060

[4] T. Suzuoki and T. Kimura, D/H and 18O/16O fractionation in ice-water system, J. Mass Spectrom. Soc. Jpn. **21**, 229–233 (1973), https://doi.org/10.5702/massspec1953.21.229

[5] R. Gragnani, M. Guglielmin, A. Longinelli, B. Stenni, C. Smiraglia, and L. Cimino, in: *Proceedings of the Seventh International Conference on Permafrost*, Collection Nordiana No 55 (Yellowknife, Canada, 1998) pp. 335–340.

[6] R. Souchez, J.-L. Tison, and J. Jouzel, Freezing rate determination by the isotopic composition of the ice, Geophys. Res. Lett. **14**(6), 599–602 (1987), https://doi.org/10.1029/GL014i006p00599

[7] L.S. Brosius, K.M. Walter Anthony, G. Grosse, J.P. Chanton, L.M. Farquharson, P.P. Overduin, and H. Meyer, Using the deuterium isotope composition of permafrost meltwater to constrain thermokarst lake contributions to atmospheric CH_4 during the last deglaciation, J. Geophys. Res. Biogeosci. **117**, G01002 (2012), https://doi.org/10.1029/2011JG001810

[8] R.L. Stotler, S.K. Frape, T. Ruskeeniemi, P. Pitkänen, and D.W. Blowes, The interglacial-glacial cycle and geochemical evolution of Canadian and Fennoscandian Shield groundwaters, Geochim. Cosmochim. Acta **76**, 45–67 (2012), https://doi.org/10.1016/j.gca.2011.10.006

[9] S.V. Alexeev and L.P. Alexeeva, Ground ice in the sedimentary rocks and kimberlites of Yakutia, Russia, Permafr. Periglac. Processes **13**(1), 53–59 (2002), https://doi.org/10.1002/ppp.408

[10] S.V. Alexeev and L.P. Alexeeva, Hydrogeochemistry of the permafrost zone in the central part of the Yakutian diamond-bearing province, Russia, Hydrogeol. J. (2003), https://doi.org/10.1007/s10040-003-0270-8

[11] S. Jessen, H.D. Holmslykke, K. Rasmussen, N. Richardt, and P.E. Holm, Hydrology and pore water chemistry in a permafrost wetland, ilulissat, Greenland, Water Resourc. Res. **50**(6), 4760–4774 (2014), https://doi.org/10.1002/2013WR014376

[12] R. Kononova, in: *Problems of Theoretical and Regional Hydrogeochemistry* (1979) pp. 119–123 [in Russian].

[13] D. Lacelle, B. Lauriol, and I.D. Clark, Effect of chemical composition of water on the oxygen-18 and carbon-13 signature preserved in cryogenic carbonates, Arctic Canada: Implications in paleoclimatic studies, Chem. Geol. **234**(1–2), 1–16 (2006), https://doi.org/10.1016/j.chemgeo.2006.04.001

[14] T. McEwen and G. Marsily, *The Potential Significance of Permafrost to the Behaviour of a Deep Radioactive Waste Repository*, SKI Technical Report 91: 8 (Swedish Nuclear Power Inspectorate SKI, 1991).

[15] A. Starinsky and A. Katz, The formation of natural cryogenic brines, Geochim. Cosmochim. Acta **67**(8), 1475–1484 (2003), https://doi.org/10.1016/S0016-7037(02)01295-4

[16] R. Mokrik and R. Vaikmäe, in: *Isotope Geochemistry Research in Baltic and Belarus* (1988) pp.133–143 [in Russian].

[17] R. Mokrik, Pecularities of the formation of the isotopic composition of underground waters on the southern slope of the Baltic shield, Geologija **19**, 16–25 (1996).

[18] R. Mokrik, *The Palaeohydrogeology of the Baltic Basin. Vendian and Cambrian* (Tartu University Press, 1997).

[19] M. Yezhova, V. Polyakov, A. Tkachenko, L. Savitski, and V. Belkina, Paleowaters of North Estonia and their influence on changes of resources and quality of fresh groundwaters of large coastal water supplies, Geologija **19**, 37–40 (1996).

[20] J. Banys, V. Juodkazis, and R. Mokrik, Regional regularities of radiocarbon distribution in groundwaters of the Baltic artesian basin, Water Res. **6**(2), 243–248 (1979) [in Russian].

[21] J. Pärn, S. Affolter, J. Ivask, et al., Redox zonation and organic matter oxidation in palaeogroundwater of glacial origin from the Baltic Artesian Basin, Chem. Geol. **488**, 149–161 (2018), https://doi.org/10.1016/j.chemgeo.2018.04.027

[22] J. Pärn, K. Walraevens, M. Camp, et al., Dating of glacial palaeogroundwater in the Ordovician-Cambrian aquifer system, northern Baltic Artesian Basin, Appl. Geochem. **102**, 64–76 (2019), https://doi.org/10.1016/j.apgeochem.2019.01.004

[23] V. Raidla, K. Kirsimäe, R. Vaikmäe, E. Kaup, and T. Martma, Carbon isotope systematics of the Cambrian-Vendian aquifer system in the northern Baltic Basin: Implications to the age and evolution of groundwater, Appl. Geochem. **27**(10), 2042–2052 (2012), https://doi.org/10.1016/j.apgeochem.2012.06.005

[24] A. Babre, A. Kalvāns, K. Popovs, I. Retiķe, A. Dēliņa, R. Vaikmäe, and T. Martma, Pleistocene age paleo-groundwater inferred from water-stable isotope values in the central part of the Baltic Artesian Basin, Isotopes Environ. Health Studies (2016), https://doi.org/10.1080/10256016.2016.1168411

[25] A. Delina, A. Kalvans, T. Saks, U. Bethers, and V. Valdis, *Highlights of Groundwater Research in the Baltic Artesian Basin* (University of Latvia, Riga, 2012).

[26] V. Raidla, J. Pärn, W. Aeschbach, et al., Intrusion of saline water into a coastal aquifer containing palaeogroundwater in the Viimsi Peninsula in Estonia, Geosciences **9**(1), 47 (2019), https://doi.org/10.3390/geosciences9010047

[27] A. Sterckx, J.M. Lemieux, and R. Vaikmäe, Representing glaciations and subglacial processes in hydrogeological models: A numerical investigation, Geofluids **2017**, 4598902 (2017), https://doi.org/10.1155/2017/4598902

[28] A. Sterckx, J.-M. Lemieux, and R. Vaikmäe, Assessment of paleo-recharge under the Fennoscandian Ice Sheet and its impact on regional groundwater flow in the northern Baltic Artesian Basin using a numerical model, Hydrogeol. J. **26**(8), 2793–2810 (2018), https://doi.org/10.1007/s10040-018-1838-7

[29] R. Vaikmäe, L. Vallner, H.H. Loosli, P.C. Blaser, and M. Juillard-Tardent, Palaeogroundwater of glacial origin in the Cambrian-Vendian aquifer of northern Estonia, Geol. Soc. London, Special Publications **189**, 17–27 (2001), https://doi.org/10.1144/GSL.SP.2001.189.01.03

[30] M. Gregorauskas, R. Mokrik, and L. Savitski, Formation of available groundwater resources on

the northern Baltic coast, Sov. Geol. **11**, 80–88 (1988) [in Russian].

[31] V. Raidla, J. Pärn, S. Schloemer, et al., Origin and formation of methane in groundwater of glacial origin from the Cambrian-Vendian aquifer system in Estonia, Geochim. Cosmochim. Acta **251**, 247–264 (2019), https://doi.org/10.1016/j.gca.2019.02.029

[32] V. Raidla, K. Kirsimäe, R. Vaikmäe, et al., Geochemical evolution of groundwater in the Cambrian-Vendian aquifer system of the Baltic Basin, Chem. Geol. **258**(3–4), 219–231 (2009), https://doi.org/10.1016/j.chemgeo.2008.10.007

[33] V. Raidla, *Chemical and Isotope Evolution of Groundwater in the Cambrian-Vendian Aquifer System in Estonia* (Tartu University Press, 2010).

[34] V. Petersell, G. Åkerblom, B.-M. Ek, M. Enel, V. Mõttus, and K. Täht, *Radon Risk Map of Estonia: Explanatory Text to the Radon Risk Map Set of Estonia at Scale of 1:500 000*, SSI Report 2005: 16 – SGU Dnr. 08-466/2002 (Geological Survey of Estonia, 2005), http://www.digar.ee/id/nlib-digar:15627

[35] R. Raudsep, in: *Geology and Mineral Resources of Estonia*, eds. A. Raukas and A. Teedumäe (Estonian Academy Publishers, Tallinn, 1997) p. 436, http://geoloogia.info/

[36] A. Soesoo, J. Vind, and S. Hade, Uranium and thorium resources of Estonia, Minerals **10**(9), 798 (2020), https://doi.org/10.3390/min10090798

[37] R. Mokrik, *The Paleohydrogeology of the Baltic Basin* (Vilnius University Publishing House, Vilnius, 2003).

[38] J. Pärn, V. Raidla, R. Vaikmäe, T. Martma, J. Ivask, R. Mokrik, and K. Erg, The recharge of glacial meltwater and its influence on the geochemical evolution of groundwater in the Ordovician-Cambrian aquifer system, northern part of the Baltic Artesian Basin, Appl. Geochem. **72**, 125–135 (2016), https://doi.org/10.1016/j.apgeochem.2016.07.007

[39] M. Forte, L. Bagnato, E. Caldognetto, S. Risica, F. Trotti, and R. Rusconi, Radium isotopes in Estonian groundwater: measurements, analytical correlations, population dose and a proposal for a monitoring strategy, J Radiol. Prot. **30**(4), 761–780 (2010), https://doi.org/10.1088/0952-4746/30/4/009

[40] R. Mokrik, E. Karro, L. Savitskaja, and G. Drevaliene, The origin of barium in the Cambrian-Vendian aquifer system, North Estonia, Est. J. Earth Sci. **58**(3), 193–208 (2009), https://doi.org/10.3176/earth.2009.3.04

[41] J. Mažeika, *Regularities of Radionuclide Migration and Transformation in Lithuanian Geological Environment*, Habitation Thesis (1999).

[42] A. Zuzevicius, J. Mažeika, and V. Baltrunas, A model of Brakish groundwater formation in the Nemunas River Valley, Geologija **60**, 63–75 (2007).

[43] J. Mažeika, T. Martma, R. Petrošius, V. Jakimavičiūtė-Maselienė, and Z. Skuratovič, Radiocarbon and other environmental isotopes in the groundwater of the sites for a planned new nuclear power, Radiocarbon **55**(3), 951–962 (2013), https://doi.org/10.2458/azu_js_rc.55.16318

[44] C. Gerber, R. Vaikmae, W. Aeschbach, et al., Using ^{81}Kr and noble gases to characterize and date groundwater and brines in the Baltic Artesian Basin on the one-million-year timescale, Geochim. Cosmochim. Acta **205**, 187–210 (2017), https://doi.org/10.1016/j.gca.2017.01.033

[45] R. Vaikmäe, T. Martma, J. Ivask, et al., *Baltic Groundwater Isotope-Geochemistry Database* (Department of Geology, Tallinn University of Technology, Tallinn, 2020), https://doi.org/10.15152/GEO.488

[46] J.-M. Punning, M. Toots, and R. Vaikmae, Oxygen-18 in Estonian natural waters, Isot. Environ. Health Stud. **23**, 232–234 (2008), https://doi.org/10.1080/10256018708623797

[47] J.-M. Punning, M. Toots, and R. Vaikmäe, in: *Proceedings of the Fourth Working Meeting, Isotopes in Nature*, ed. G. Strauch (Central Institute of Isotope and Radiation Research, Leipzig, 1987) pp. 542–552.

[48] T. Weißbach, *Noble Gases in Palaeogroundwater of Glacial Origin in the Cambrian-Vendian Aquifer System, Estonia*, Master's Thesis, University of Heidelberg (Heidelberg, 2014), 116 pp.

[49] A.I. Malov, Evolution of uranium isotopic compositions of the groundwater and rock in a sandy-

clayey aquifer, Water **9**(12), 910 (2017), https://doi.org/10.3390/w9120910

[50] A.I. Malov and I.V. Tokarev, Using stable isotopes to characterize the conditions of groundwater formation on the eastern slope of the Baltic Shield (NW Russia), J. Hydrol. **578**, 124130 (2019), https://doi.org/https://doi.org/10.1016/j.jhydrol.2019.124130

[51] A.I. Malov, I.N. Bolotow, O.S. Pokrovsky, et al., Modeling past and present activity of a subarctic hydrothermal system using O, H, C, U and Th isotopes, Appl. Geochem. **63**, 93–104 (2015), https://doi.org/10.1016/j.apgeochem.2015.07.003

[52] IAEA, *Isotope Methods for Dating Old Groun*dwater (IAEA, Vienna, 2013), https://www-pub.iaea.org/MTCD/Publications/PDF/Pub1587_web.pdf

[53] S.J. Goldstein and C.H. Stirling, Techniques for measuring uranium-series nuclides 1992–2002, Rev. Miner. Geochem. **52**, 23–57 (2003).

[54] G. Bondarenko, I. Gudzenko, and N. Kovalyukh, *Formation of Radioactive and Stable Isotope Front in Disharge Area of Artesian Basin* (Nauka, 1981) pp. 157–164 [in Russian].

[55] V. Juodkazis and K. Tibar, Helium in groundwater on the northern flank of the Baltic Artesian Basin, Int. Geol. Rev. **31**(7), 736–743 (1989).

[56] R. Mokrik, V. Puura, T. Floden, and R. Petkevičius, Peculiarities of helium distribution in the Baltic Basin, Litosfera **6**, 121–123 (2002).

[57] J.L. Druhan, S.T. Brown, and C. Huber, Isotopic gradients across fluid-mineral boundaries, Rev. Mineral. Geochem. **80**(1), 355–391 (2015), https://doi.org/10.2138/rmg.2015.80.11

[58] K. Kigoshi, Alpha-recoil thorium-234: Dissolution into water and the uranium-234/uranium-238 disequilibrium in nature, Science **173**(3991), 47–48 (1971), https://doi.org/10.1126/science.173.3991.47

[59] P.I. Chalov, *Isotopic Fractionation of Natural Uranium* (Frunze, Ilim, 1975) [in Russian].

[60] V.V. Cherdyncev and P.I. Chalov, in: *Discoveries in USSR* (Moscow, 1977) pp. 28–31 [in Russian].

[61] J.K. Osmond and J.B. Cowart, The theory and uses of natural uranium isotopic variations in hydrology, Atom. Energy Rev. **14**(4), 621–679 (1976), https://inis.iaea.org/search/search.aspx?orig_q=RN:8327949

[62] M.B. Andersen, C.H. Stirling, D. Porcelli, A.N. Halliday, P.S. Andersson, and M. Baskaran, The tracing of riverine U in Arctic seawater with very precise $^{234}U/^{238}U$ measurements, Earth Planet. Sci. Lett. **259**(1–2), 171–185 (2007), https://doi.org/10.1016/j.epsl.2007.04.051

[63] L.F. Robinson, N.S. Belshaw, and G.M. Henderson, U and Th concentrations and isotope ratios in modern carbonates and waters from the Bahamas, Geochim. Cosmochim. Acta **68**(8), 1777–1789 (2004), https://doi.org/10.1016/j.gca.2003.10.005

[64] R.L. Fleischer and O.G. Raabe, Recoiling alpha-emitting nuclei. Mechanisms for uranium-series disequilibrium, Geochim. Cosmochim. Acta **42**(7), 973–978 (1978), https://doi.org/https://doi.org/10.1016/0016-7037(78)90286-7

[65] V.E. Lee, D.J. DePaolo, and J.N. Christensen, Uranium-series comminution ages of continental sediments: Case study of a Pleistocene alluvial fan, Earth Planet. Sci. Lett. **296**(3–4), 244–254 (2010), https://doi.org/10.1016/j.epsl.2010.05.005

[66] M.B. Andersen, Y. Erel, and B. Bourdon, Experimental evidence for ^{234}U-^{238}U fractionation during granite weathering with implications for $^{234}U/^{238}U$ in natural waters, Geochim. Cosmochim. Acta **73**(14), 4124–4141 (2009), https://doi.org/10.1016/j.gca.2009.04.020

[67] E. Yakovlev, G. Kiselev, S. Druzhinin, and S. Zykov, Uranium isotopic fractionation (234U, 238U) in the formation of ice crystals, Vestnik of Northern (Arctic) Federal University. Series Natural Sciences **3**, 15–23 (2016) [in Russian], https://doi.org/10.17238/issn2227-6572.2016.3.15

[68] S.T. Brown, A. Basu, J.N. Christensen, P. Reimus, J. Heikoop, A. Simmons, G. Woldegabriel, K. Maher, K. Weaver, J.T. Clay, and D. LePaolo, Isotopic evidence for reductive immobilization of uranium across a roll-front mineral deposit, Environ. Sci. Technol. **50**(12), 6189–6198 (2016), https://doi.org/10.1021/acs.est.6b00626

[69] J.K. Osmond and J.B. Cowart, in: *Uranium-series Disequilibrium: Applications to Earth, Marine, and Environmental Sciences*, 2nd ed., eds. M. Ivanovic and R.S. Harmon (Clarendon Press,

Oxford, 1992), http://inis.iaea.org/search/search.aspx?orig_q=RN:25065862

[70] M. Gascoyne, in: *Uranium-series Disequilibrium: Applications to Earth, Marine, and Environmental Sciences*, 2nd ed., eds. M. Ivanovic and R.S. Harmon (Clarendon Press, Oxford, 1992), http://inis.iaea.org/search/search.aspx?orig_q=RN:25065862

[71] J.N. Andrews, I.S. Giles, R.L.F. Kay, D.J. Lee, J.K. Osmond, J.B. Cowart, P. Fritz, J.F. Barker, and J. Gale, Radioelements, radiogenic helium and age relationships for groundwaters from the granites at Stripa, Sweden, Geochim. Cosmochim. Acta **46**(9), 1533–1543 (1982), https://doi.org/https://doi.org/10.1016/0016-7037(82)90312-X

[72] M.A. Walvoord and B.L. Kurylyk, Hydrologic impacts of thawing permafrost – A review, Vadose Zone J. **15**(6), 1–20 (2016), https://doi.org/10.2136/vzj2016.01.0010

[73] B.L. Kurylyk, K.T.B. MacQuarrie, and J.M. McKenzie, Climate change impacts on groundwater and soil temperatures in cold and temperate regions: Implications, mathematical theory, and emerging simulation tools, Earth Sci. Rev. **138**, 313–334 (2014), https://doi.org/10.1016/j.earscirev.2014.06.006

[74] P. Glynn, C. Voss, and A. Provost, in: *Use of Hydrological Information in Testing Groundwater Flow Models: Technical Summary and Proceedings of a Workshop*, Borgholm, Sweden, September 1–3, 1997 (Nuclear Energy Agency, Issy-les-Moulineaux, 1999) pp. 201–241, https://www.etde.org/etdeweb/details_open.jsp?osti_id=342806

[75] O. Landström, E.-L. Tullborg, G. Eriksson, and Y. Sandell, *Effects of Glacial/Post-glacial Weathering Compared with Hydrothermal Alteration – Implications for Matrix diffusion. Results from Drillcore Studies in Porphyritic Quartz Monzodiorite from Äspö SE Sweden*, SKB Rapport R-01-37 (SKB, Stockholm, 2001).

[76] P. Mejean, D.L. Pinti, B. Ghaleb, and M. Larocque, Fracturing-induced release of radiogenic ^{4}He and ^{234}U into groundwater during the last deglaciation: An alternative source to crustal helium fluxes in periglacial aquifers, J. Am. Water Resourc. Assoc. **53**(7), 5677–5689 (2017), https://doi.org/10.1002/2016WR020014

[77] G.P. Kiselev, E.Y. Yakovlev, S.V. Druzhinin, and A.S. Galkin, Distribution of radioactive isotopes in rock and ore of Arkhangelskaya pipe from the Arkhangelsk diamond province, Geol. Ore Dep. **59**(5), 391–406 (2017), https://doi.org/10.1134/S1075701517050014

[78] V.I. Ferronsky and V.A. Polyakov, *The Hydrosphere Isotopes* (Nauka Publishing House, Moscow, 1983) [in Russian].

[79] M.E. Räsänen, J.V. Huitti, S. Bhattarai, J. Harvey, and S. Huttunen, The SE sector of the Middle Weichselian Eurasian Ice Sheet was much smaller than assumed, Quat. Sci. Rev. **122**, 131–141 (2015), https://doi.org/10.1016/j.quascirev.2015.05.019

[80] V. Kalm, A. Raukas, M. Rattas, and K. Lasberg, in: *Quaternary Glaciations – Extent and Chronology*, eds. J. Ehlers, P. L. Gibbard, P.D. Hughes, Devel. Quatern. Sci. **15**, 95–104 (2011), https://doi.org/10.1016/B978-0-444-53447-7.00008-8

[81] R. Mokrik, V. Samalavičius, M. Bujanauskas, and M. Gregorauskas, Environmental isotopes and noble gas ages of the deep groundwater with coupled flow modelling in the Baltic artesian basin, Lith. J. Phys. **61**(1), 53–65 (2021), https://doi.org/10.3952/physics.v61i1.4407

[82] R. Mokrik, L. Savitskaja, and L. Savitski, Aqueous geochemistry of the Cambrian–Vendian aquifer system in the Tallinn intake, northern Estonia, Geologija **51**(3), 50–56 (2005), https://mokslozurnalai.lmaleidykla.lt/geologija/2005/3/2867

[83] M. Zhang and S.K. Frape, *Permafrost: Evolution of Shield Groundwater Compositions During Freezing*, Ontario Power Generation Report 06819-REP-01200-10098-R00 (Toronto, 2003).

[84] B. Herut, A. Starinsky, A. Katz, and A. Bein, The role of seawater freezing in the formation of subsurface brines, Geochim. Cosmochim. Acta **54**(1), 13–21 (1990), https://doi.org/10.1016/0016-7037(90)90190-V

[85] M.A. McCaffrey, B. Lazar, and H.D. Holland, The evaporation path of seawater and the coprecipitation of Br^- and K^+ with halite, J. Sediment. Res. **57**(5), 928–937 (1987), https://doi.org/10.1306/212f8cab-2b24-11d7-8648000102c1865d

ŠIAURINĖS BALTIJOS REGIONO POŽEMINIO VANDENS CHEMINĖS SUDĖTIES IR $^{234}U/^{238}U$ IZOTOPŲ SANTYKIO PUSIAUSVYROS ANOMALIJOS INTERPRETACIJA

R. Mokrik, V. Samalavičius

Vilniaus universiteto Geomokslų institutas, Vilnius, Lietuva

Santrauka

Estijos kambro–vendo (ediakaro) (Cm-V) ir ordoviko–kambro (O-Cm) vandeninguose sluoksniuose yra aptinkamas anomalios izotopinės ir cheminės sudėties požeminis vanduo, susiformavęs pleistoceno laikotarpiu. Minėti vandeningi sluoksniai ir viršutinė kristalinio pamato dalis buvo hidrauliškai susieti periglacialinėje aplinkoje ir sudarė vieningą hidrogeologinę sistemą. Požeminio vandens sudėtis buvo reikšmingai pakeista vykstant izotopiniam ir geocheminiam frakcionavimuisi dėl užšalimo. Šiame tyrime panaudotas urano izotopų santykis ($^{234}U/^{238}U$), helio koncentracija, izotopinė ir cheminė sudėtis ir koreguotas ^{14}C amžius siekiant iš naujo įvertinti šiaurinės Baltijos baseino dalies požeminio vandens evoliuciją. Urano izotopų santykio ir mineralizacijos diagrama leido naujai nustatyti kraštinių narių (Baltijos jūros, modernaus ir *in situ* sluoksnio vandens) įtaką Talino srityje esančio požeminio vandens formavimuisi. Vandens amžiaus rezultatų ir urano santykių analizė atskleidė, kad požeminis vanduo buvo ilgai veikiamas periglacialinės aplinkos, todėl įvyko jo sudėties pokyčiai. Stabiliųjų izotopų ($\delta^{18}O$ ir δD) ir hidrogeocheminiai parametrai indikuoja kriogeninę vandens kilmę.

Pagrindiniai veiksniai, lėmę požeminio vandens anomalijų atsiradimą pleistoceno laikotarpiu, yra daugiamečio įšalo sukelta izotopinės ir cheminės sudėties kaita, periodiška mitybos ir iškrovos zonų inversija, jūros ir periglacialinių ežerų lygio svyravimai, skirtingos kilmės vandenų maišymasis talikuose ir kristaliname pamate. Dėl šių procesų susidaro specifinė vandens cheminių tipų seka ir zoniškumas, taip pat dvi atskiros požeminio vandens frakcijos – apatinė koncentruota ir viršutinė nugėlinta. Požeminio vandens eksploatacija destabilizavo natūralią pusiausvyros būseną, susidariusią holoceno ir pleistoceno laikotarpiais.